Mutation and Evolution of the Magnesium-Binding Site of a Class II Aminoacyl-tRNA Synthetase†

Laurent Ador,‡ Sophie Jaeger,‡ Renaud Geslain,‡ Franck Martin,‡ Jean Cavarelli,§ and Gilbert Eriani*,‡

UPR 9002 SMBMR du CNRS, Institut de Biologie Moléculaire et Cellulaire, 15, rue René Descartes, 67084 Strasbourg, France, and UMR7104 Département de Biologie et Génomique Structurales, IGBMC, CNRS, INSERM, ULP, 1, rue Laurent Fries, BP163, 67004 Illkirch, France

Received February 24, 2004; Revised Manuscript Received April 5, 2004

ABSTRACT: Aminoacyl-tRNA synthetases contain one or three Mg^{2+} ions in their catalytic sites. In addition to their role in ATP binding, these ions are presumed to play a role in catalysis by increasing the electropositivity of the α-phosphate and stabilizing the pentavalent transition state. In the class II aaRS, two highly conserved carboxylate residues have been shown to participate with Mg^{2+} ions in binding and coordination. It is shown here that these carboxylate residues are absolutely required for the activity of *Saccharomyces cerevisiae* aspartyl-tRNA synthetase. Mutants of these residues exhibit pleiotropic effects on the kinetic parameters suggesting an effect at an early stage of the aminoacylation reaction, such as the binding of ATP, Mg^{2+}, aspartic acid, or the amino acid activation. Despite genetic selections in an *APS*-knockout yeast strain, we were unable to select a single active mutant of these carboxylate residues. Nevertheless, we isolated an intragenic suppressor from a combinatorial library. The active mutant showed a second substitution close to the first one, and exhibited a significant increase of the tRNA aminoacylation rate. Structural analysis suggests that the acceptor stem of the tRNA might be repositioned to give a more productive enzyme:tRNA complex. Thus, the initial defect of the activation reaction was compensated by a significant increase of the aminoacylation rate that led to cellular complementation.

Aminoacyl-tRNA synthetases (aaRS)[1] are key players in one of the early steps of the translation of the genetic information. These enzymes catalyze the formation of aminoacyl-tRNAs in a two-step reaction, starting by the activation of the amino acid by ATP in the presence of magnesium ions followed by the transfer of the amino acid moiety to the tRNA. Each aaRS is specific to one amino acid and to one or several tRNA isoacceptors. AaRS constitute one of the most documented examples where the same catalytic reaction is performed on two different structural platforms, each of them being characterized by the exclusive motifs and biochemical features (*1*). The class I and class II aaRS aminoacylate the 2′-OH and the 3′-OH of the 3′-terminal ribose, respectively. Although the strategy for the specific amino acid and tRNA recognition is unique to each synthetase, the mechanisms of the two catalytic steps are essentially conserved among the 20 aaRS. The first step of the aminoacylation reaction, the activation of amino acid, proceeds through an in-line nucleophilic displacement mechanism with the formation of a pentacoordinate phosphorus transition state. The second step, or transfer of the amino acid to the tRNA, proceeds through the formation of a tetrahedral intermediate formed during the nucleophilic attack on the carbonyl carbon of the adenylate by the oxygen of the 2′- or 3′-OH of the Ade76 (*2*−*4*). In addition to the three substrates, aaRS bind magnesium as cofactor. Mg^{2+} ions contribute to ATP binding and presumably play a role in the stabilization of the pentavalent transition state by interacting with the highly charged α-phosphate. They may also play a role in the release of the pyrophosphate moiety of ATP, and more generally, they are involved in tRNA structure stabilization.

Aspartyl-tRNA synthetase (AspRS) is one of the 10 class II aaRS. Of the 20 aminoacyl-tRNA synthetases, AspRS is probably the one with the greatest amount of available structural data. Up to now, the aspartic system is the only one for which at least one example of three-dimensional (3D) structure in each kingdom has been described. The first determined class II aaRS in complex with the cognate tRNA was from the eukaryote *Saccharomyces cerevisiae* (*5*). Following this, the ternary complex AspRS:$tRNA^{Asp}$:ATP was solved (*4*). The first observation of an aminoacyl-adenylate formed as a cocrystal was made using the *Thermus thermophilus* enzyme (*6*). More recently, a complete picture of the interactions with the small substrates, divalent ions, and adenylate intermediate was drawn for the archaeal AspRS from *Pyrococcus kodakaraensis* KOD. With the tRNA, several homologous complexes have been solved (*2*,

† This work was supported by the Centre National de la Recherche Scientifique, and grants from Union Européenne (4ème Programme des Biotechnologies ≪ Design of RNA Domains, Substrates or Inhibitors of tRNA Recognizing Proteins ≫).

* Corresponding author: G. Eriani, UPR 9002 SMBMR du CNRS, Institut de Biologie Moléculaire et Cellulaire, 15, rue René Descartes, 67084 Strasbourg, France. Tel.: 33 3.88.41.70.42; Fax: 33 3.88.60.22.18; E-mail: G.Eriani@ibmc.u-strasbg.fr.

‡ UPR 9002 SMBMR du CNRS, Institut de Biologie Moléculaire et Cellulaire.

§ UMR7104 Département de Biologie et Génomique Structurales, IGBMC, CNRS, INSERM.

[1] Abbreviations: aaRS, aminoacyl-tRNA synthetase; *APS*, AspRS gene; 5-FOA, 5-fluoro-orotic acid; 3D, three-dimensional.

10.1021/bi049617+ CCC: $27.50
Published on Web 05/11/2004

7, 8) as well as two heterologous complexes that contribute to the understanding of the tRNA binding mechanism and the specificity (*8, 9*). Surprisingly, crystals of the apoenzyme were only obtained recently, and simultaneous resolution of the yeast and *Escherichia coli* AspRS free of any substrate was obtained (*10, 11*). The scope of these structures was to provide a reference structure, unperturbed by ligand binding, to ascertain the structural changes caused by ligand interactions (*11*). All together, these data provide a thorough view on the substrates binding and on the catalytic mechanisms. The aspartyl-adenylate molecule lies at the bottom of the catalytic domain, stretched on the antiparallel β-sheet and held in place by a network of interactions belonging principally to class II motifs 2 and 3 and to an AspRS invariant LXQ(S/A)PQXXKQ sequence preceding motif 2, more involved in the aspartate moiety binding (*2*, *9*, *12*). In contrast to the linear shape of the aspartyl-adenylate molecule, the ATP molecule adopts the class II-specific U-shaped conformation, with the pyrophosphate moiety of the molecule bent toward the adenine ring (*4*, *12*−*14*). The superimposition of the catalytic sites of the different AspRS complexes shows the strict conservation of the position and conformation of the aspartyl-adenylate. Moreover, the ATP and aspartic acid substrates individually have been shown to be superimposed on their corresponding counterparts in the aspartyl-adenylate complex (*12*); this also remains true even in the presence of the tRNA (*2*). This suggests that only subtle changes in enzyme residues and ligands are responsible for the stabilization of the transition states of both activation and acylation reactions. Nevertheless, the class II active site is not a static partner of the aminoacylation reaction, and several peptides of the active site display high mobility as suggested by the different conformations adopted in the different complexes. Two mobile loops called "flipping loop" and "histidine loop" have been defined. The position of these loops depend of the nature of the substrates bound to the enzyme, but both are involved in maintaining the aspartic acid or adenylate bound in its proper conformation (for a discussion see refs *2* and *12*).

In the present work, we investigate the functional importance of two acidic residues that are invariably found into the catalytic site of all AspRS sequences. These residues participate in the stabilization of the U-shaped conformation of ATP by their interactions with the Mg^{2+} ions. In class II synthetases, three hexacoordinated Mg^{2+} ions stabilize the bent conformation of ATP. One is located between the α- and β-phosphates of ATP, and the other two are on both sides of the β- and γ-phosphates. The hexacoordination of the Mg^{2+} ions is completed with water molecules and several well-conserved residues such as the two acidic residues examined here. In a previous study, we have shown that conservative changes or Ala substitutions of these acidic residues drastically reduced the enzyme activity (*4*). Here, we extend this investigation with degenerated libraries of AspRS mutants that were screened in vivo in an *APS*-knockout strain. In the first step, we showed, by saturation mutagenesis, that the two acidic residues could not be substituted without giving a lethal phenotype. In the second step, we statistically degenerated the peptidic region surrounding the acidic residues to isolate active suppressors of the lethal mutations. This way, we were able to suppress the lethal effect by a distal mutation that modifies the tRNA acceptor stem binding and gives a more productive enzyme: tRNA complex. A significant increase of the aminoacylation rate was therefore observed, which led to cell growth.

EXPERIMENTAL PROCEDURES

Bacterial, Yeast Strains, and Shuttle Vectors. E. coli TB1 (F$^-$ *ara* Δ*(lac-proAB) hsdR* (r_k^- m_k^+) *rpsL(Str^r) [ϕ80, dlac*Δ*(lacZ)M15]*) was used as a recipient for cloning procedures. *E. coli* TAP56 (*leu thi hsdR rpsL supE* Δ*lacU169 galK$_{am}$ (λkil cI857*Δ*bioA)*) was the host strain of pTG908 harboring the *APS* gene. It was kindly provided by D. L. Court (*15*).

The AspRS disrupted haploid strain *S. cerevisiae* YALG4 (*a ura3*−*52 lys2*−*801^{am} trp1*-Δ*63 his3*-Δ*200 leu2*-Δ*1 ade2*-Δ*450 ade3*-Δ*1483 aps::HIS3*) was used to select the active and inactive *APS* genes (*16*). YAL3 is a derivative of YALG4 transformed by pAL3 (see below).

Plasmid pAL3 was constructed by cloning the 3.8-kbp DNA fragment encoding *APS* (*17*) into pALR10 (pUN50-*ADE3*); the resulting plasmid is Ura$^+$, Ade3$^+$, APS$^+$. Plasmid pEG93 is a yeast centromeric vector derived of pBR322 in which the *TRP1* marker, the *ARS-CEN* and the *APS* genes were cloned in the *Sal*I, *Cla*I, and *Bam*HI restriction sites, respectively. pRS314-*APS* contains the *APS* gene between the *Sal*I−*Sma*I sites of pRS314 (*18*), the resulting vector is Trp$^+$, APS$^+$. Plasmid pGALS1315-*APS* (*LEU2*, *ADE3*, *Kan^R*, *GALS$_{(operator)}$APS*) is a derivative of pRS315 carrying a truncated form of the GAL1 promoter in front of the *APS* gene (*19*). This promoter allows a tight control of the *APS* expression, with a total repression in the presence of glucose and moderate expression in the presence of the natural inducer galactose (*19*). To easily isolate this vector from yeast strains harboring other vectors carrying the β-lactamase gene, the *bla* gene was replaced by a kanamycin resistance cassette from pBSL15 (*20*). An additional marker *ADE3* was inserted to confer a red coloration to the *ade2* yeast strains (*21*). The bacterial and yeast strains were grown and transformed according to standard procedures (*22*).

Oligonucleotide Directed Site-Specific Mutagenesis. Oligonucleotides were synthesized by Genset (Paris, France) and IBA-NAPS (Göttingen, Germany). Oligonucleotides for saturating mutagenesis were the following: D471F472: 5′-TCACCCCTCATGAA*NNNNNN*ATACGAGTTACAAT-3′, E478I479: 5′-TGTGCACCGGACAA*NNNNNN*TTCAC-CCCTCATGA-3′ where *N* represents an equimolar mixture of the four deoxynucleotides. The oligonucleotides used for the selection of suppressors corresponded to the gene segment encoding peptide N468 to Q484. All the positions contained 90% of the native nucleotide and 10% of an equimolar mixture of the four deoxynucleotides.

Mutagenesis was performed according to ref *23* with the uracil-containing single-stranded DNA from pRS314-*APS* as template or pRS314-*APS*$_{(DA471,DN471\ or\ EG478)}$. The resulting libraries each contained about 20 000 clones. The mutated AspRS genes were subcloned as *Sac*I−*Mlu*I DNA fragments into the *E. coli* expression vector pTG908-*APS* (*24*).

Phenotypic Selection of APS Genes Based on Plasmid Shuffle Assays. Two in vivo assays were used to analyze the effect of mutated *APS* on the yeast cell growth. The first was a colored assay based on the change of the color of colonies (*21*). The second was a positive selection assay based on the resistance to 5-FOA (5-fluoro-orotic acid) (*25*).

In the colored assay, the YAL3 strain was transformed with the mutated pRS314-*APS* vectors and plated on minimal medium supplemented with adenine (limiting concentration of 2 μg mL^{-1}), with histidine (20 μg mL^{-1}), with uracil (20 μg mL^{-1}), with lysine (20 μg mL^{-1}), and with leucine (60 μg mL^{-1}). A concentration of 50 ng of DNA was found to be optimal to obtain about 200 isolated colonies per 88-mm-diameter Petri dishes. After a 72 h incubation at 30 °C, the red nonsectored coloration (Sect$^-$) was observed in case of inactive *APS* (*16*).

In the 5-FOA assay, the cells were subjected to a drop test on minimal medium containing 5-FOA (4×10^{-3} M) (Toronto Research Chemicals, Canada), adenine (10 μg mL^{-1}), histidine (20 μg mL^{-1}), uracil (25 μg mL^{-1}), lysine (20 μg mL^{-1}), and leucine (60 μg mL^{-1}). In case of inactive *APS*, pAL3 cannot leave the cell and *URA3* eventually metabolizes the 5-FOA into 5-FUMP (5-fluoro-UMP), which is toxic for the cell.

By these two methods, we were able to identify the yeast cells that contain active *APS* genes from those that contained inactive *APS* genes.

Selection of APS Genes with the GALS Promoter. The GALS promoter is an upstream activating sequence-truncated GAL1 promoter that is totally repressed on glucose medium. This efficient repression allowed us to build a conditional strain for *APS*. When cloned behind the GALS promoter, the *APS* gene was controlled by glucose/galactose growth conditions (*19*). Consequently, a yeast strain disrupted for *APS* (*aps::HIS3*), rescued by a *GALS*$_{(operator)}$*APS*, is able to grow in galactose-containing medium while it is unable to grow in glucose-containing medium. This conditional strain allowed us to assay large libraries of degenerated *APS* present in a pRS314-type vector. This system of positive selection was particularly powerful for the detection of active suppressors of *APS*.

In the first step, YAL3 strain (YALG4, pAL3) was transformed by pGALS1315-*APS*, and the resident pAL3 vector was shuffled on 5-FOA and galactose-containing medium. The resulting YALG4-pGALS1315-*APS* strain was ready to be transformed by the libraries of mutated pRS314-*APS*. Transformants were plated on glucose-containing media to switch off the expression of *APS* from the rescuing pGALS1315-*APS*. Clones that were growing contained active AspRS encoded by pRS314-*APS*. Then, the plasmids were extracted from the yeast cells, and the mutations were identified by DNA sequencing.

AspRS Overexpression and Purification. Plasmid pTG908 was used to overexpress the yeast AspRS in *E. coli*. It contains the λ P_L promoter, which allows high level expression of native and mutated genes of AspRS after heat induction (*26*, *27*). The mutated *APS* alleles were introduced into the vector pTG908 by replacement of the 1.85-kbp DNA fragment *Sac*I−*Mlu*I of pTG908-*APS*. The strain TAP56 was transformed with these constructions, grown, and induced according to ref *15*. Purification of the AspRS proteins was performed in one fractionation step by HPLC on a hydroxyapatite column (Progel TSK HA-1000) according to ref *28*.

Measurement of Kinetic Parameters. tRNA^{Asp} aminoacylation, ATP-PPi exchange reaction and determination of k_{cat} and K_m values were performed as described previously (*29*). Total yeast tRNA were obtained from Boehringer Mannheim (Germany) and [^{14}C]L-aspartic acid was obtained from the CEA (Saclay, France). For K_m measurements, the substrate concentrations varied from 0.25 to 2 K_m values. The K_d of AspRS for [^{32}P]-labeled tRNA^{Asp} was determined by the nitrocellulose filtration method with various enzyme concentrations extending from 10^{-8} to 10^{-6} M (*28*).

Table 1: Growth Phenotypes in the AspRS-Knockout Strain and k_{cat} for the Aminoacylation and ATP-PPi Exchange Reaction[a]

	growth phenotype	aminoacylation		ATP-PPi exchange		K_d
		k_{cat} s^{-1}	K_m ATP μM	k_{cat} s^{-1}	K_m Asp mM	tRNA^{Asp} 10^{-8} M
wild-type	viable	0.83	30	27	2.5	3.0
DE471	lethal	0.007	1750	6.1	19.6	2.7
DN471	lethal	0	nd	1.3	43.5	nd
DA471	lethal	0	nd	0	nd	5.0
ED478	lethal	0	nd	0	nd	3.0
EQ478	lethal	0	nd	0	nd	nd
EA478	lethal	0	nd	0	nd	nd

[a] The growth phenotype was determined on 5-FOA-containing medium. Aminoacylation and ATP-PPi exchange data are from ref *4*. nd, not determined.

RESULTS

Mutation of the Two Acidic Residues Inactivates AspRS and Leads to Cell Lethality. D471 and E478 have been previously mutated (*4*). Despite conservative changes, the six mutant enzymes (DA471, DN471, DQ471, EA478, ED478, EQ478) were inactive or exhibited less than 1% of aminoacylation activity. Decreases of the amino acid activation and increases of the K_m for ATP and aspartate were concomitantly observed (Table 1). Thus, these effects contribute to show the importance of the two acidic residues for the enzyme activity. The quasi invariance of these residues in class II synthetases reinforces the idea of a conservative function for these couple of interactions between the Mg^{2+} ions and the protein residues.

Consecutively to this first in vitro approach, we cloned six mutants in the shuttle plasmid pEG93 and assay the in vivo activity of the mutated genes by a shuffle test on 5-FOA in the yeast strain YAL3. Of the six mutants, none were able to grow on 5-FOA, which means that none of the mutated AspRS were active enough to substitute for the native AspRS encoded by the rescuing plasmid (Table 1). Cell death followed the metabolism of 5-FOA by the product of *URA3* present on the rescuing plasmid.

Search for Active Variants of the Two Acidic Residues. To extend our initial analyses, we had two main goals. The first one was to look for amino acid substitution of residues D471 and E478 which could lead to an active AspRS. The second one was to discover double mutants which could compensate the previously observed lethal effect (*4*) and which might recover the catalytic activity. Therefore, we searched for viable variants of residues 471 and 478 in an exhaustively mutated library and tried to isolate compensatory mutations of the initial mutation.

We used a positive selection of active AspRS based on the galactose-inducible AspRS yeast strain. For this, we used an *APS*-knockout strain (YAL3) rescued by an AspRS expressed from pGALS1315-*APS* on galactose containing medium. Two combinatorial libraries of pRS314-*APS*, mutated at saturation of the 471−472 and 478−479 residues, were screened in the knockout strain on glucose-containing

medium. Glucose strongly represses the GALS promoter, leading to a progressive decrease and arrest of AspRS expression from pGALS1315-*APS*. Thus, the yeast growth becomes strictly dependent on the AspRS activity resulting from pRS314-*APS*. In the two libraries, the acidic residues were mutated together with the adjacent residues (D471 with F472 and E478 with I479, respectively).

The adjacent residues exhibited significant variation in the different AspRS sequences, and thus they might vary and serve as internal control for the efficiency of mutagenesis. We also made the assumption that the mutation of these residues may induce some structural changes able to compensate for the lethal effect. Several thousands of mutated plasmids were screened on the glucose-containing plates. In the first attempt, we isolated hundreds of colonies containing the native sequence. This was explained by the low efficiency of the Kunkel mutagenesis that was performed on a native template of *APS* (pRS314-*APS*). The resulting library was biased toward the wild-type sequence. To circumvent this problem, we prepared in a second attempt, two libraries derived from lethal mutants of *APS*. One library was built with a lethal DA471 mutant, to screen positions 471−472, and the other on the EG478 mutant (*16*), to screen the positions 478−479. In other words, the clones isolated from these two templates were true revertants or second site-revertants (pseudo-revertants) of the lethal mutations located at the 471 and 478 positions. To verify that the colony growth resulted from the shuffle of the pGALS1315-*APS* plasmid, we also checked the coloration of the colonies. We used the property of the *ADE3* marker that gives a red coloration in an *ade2*$^-$ background. The expected colony phenotype for an active revertant of the lethal mutations encoded by pRS314-*APS*$_{(DA471\ or\ EG478)}$ was red with white sectors. It resulted from the progressive loss of the pGALS1315-*APS* plasmid that occurred when the cell growth was sustained by the AspRS originating from pRS314-*APS*. The red-white sectored phenotype guaranteed the correct shuffling of the original pGALS1315-*APS* plasmid. Following the colony isolation, total DNA was extracted from the yeast cells and the plasmid DNA from pRS314-*APS* was isolated after transformation of *E. coli* cells. Phenotypes were confirmed by a second cycle of transformation and selection in the (YAL3, pGALS1315-*APS*) strain. Then, the mutations were identified by DNA sequencing.

We screened about 1500 plasmids in both libraries. As most of the plasmids did not give a viable phenotype, we determined this number on galactose-containing plates. Forty-two clones containing active revertants were isolated starting from the *APS*$_{(DA471)}$ library and 54 from the *APS*$_{(EG478)}$ library (Tables 2 and 3). Twenty-one and 12 clones respectively were true revertants of the two lethal mutations; they contained the native DNA sequence or a silent mutation. In the *APS*$_{(DA471)}$ library, the other 21 clones contained reversions of the Ala lethal mutation in the original aspartate residue. However, residue 472 exhibited changes in Gly, Leu, Ser, Cys, Tyr, and Trp. Whereas D471 is strictly conserved in all AspRS sequences, residue 472 is frequently changed to Leu, Met, Ile, or Val. Here, we show that small polar residues can also be used at this level of the protein. However, we do not know if the catalytic performances of the mutants are affected by the mutations, we only expect that they are maintained above the threshold necessary for cell growth. In *APS*$_{(EG478)}$ library, the other 42 mutants exhibited, in all cases, a reversion of the lethal G478 mutation in the original E478 residue. The mutants were characterized by variations of the adjacent F479 residue. Although the AspRS sequences exhibited few variations of this residue and a marked hydrophobic character (Ile, Leu, Val, and Met residues are only found), we observed 12 different residues with distinct chemical properties (Tables 2 and 3). Here also, we do not know if the catalytic properties were affected by these mutations.

Table 2: Sequences of the Selected Revertants, of the Original Lethal Mutant, and of the Native Protein[a]

wild-type sequence	$D_{471}F_{472}$	gat ttc	
lethal used for the selection	$A_{471}F_{472}$	gct ttc	
wild-type revertants	$D_{471}F_{472}$	gAt ttc	(14)
	$D_{471}F_{472}$	gAt ttT	(4)
	$D_{471}F_{472}$	gAC ttc	(3)
mutated revertants	$D_{471}\mathbf{L}_{472}$	gAt ttG	(1)
	$D_{471}\mathbf{L}_{472}$	gAt ttA	(4)
	$D_{471}\mathbf{L}_{472}$	gAC Ctc	(1)
	$D_{471}\mathbf{G}_{472}$	gAC GGc	(4)
	$D_{471}\mathbf{G}_{472}$	gAt GGc	(5)
	$D_{471}\mathbf{G}_{472}$	gAt GGG	(1)
	$D_{471}\mathbf{S}_{472}$	gAt tCc	(1)
	$D_{471}\mathbf{C}_{472}$	gAC tGc	(1)
	$D_{471}\mathbf{Y}_{472}$	gAt tAc	(2)
	$D_{471}\mathbf{W}_{472}$	gAt tGG	(1)

[a] The amino acid residues that differ from the native sequence are in bold underlined. DNA sequences follow. Nucleotides in capitals indicate the changes compared to the lethal template used to prepare the library. Number between brackets referred to the number of clones selected.

Table 3: Sequences of the Selected Revertants, of the Original Lethal Mutant, and of the Native Protein[a]

wild-type sequence	$E_{478}I_{479}$	gaa atc	
lethal used for the selection	$G_{478}I_{479}$	gga atc	
wild-type revertants	$E_{478}I_{479}$	gAa atc	(8)
	$E_{478}I_{479}$	gAa atT	(1)
	$E_{478}I_{479}$	gAG atc	(3)
mutated revertants	$E_{478}\mathbf{S}_{479}$	gAa aGT	(2)
	$E_{478}\mathbf{S}_{479}$	gAG aGc	(1)
	$E_{478}\mathbf{S}_{479}$	gAa TCT	(1)
	$E_{478}\mathbf{S}_{479}$	gAa TCc	(5)
	$E_{478}\mathbf{S}_{479}$	gAa TCA	(2)
	$E_{478}\mathbf{S}_{479}$	gAG TCC	(1)
	$E_{478}\mathbf{N}_{479}$	gAG aAc	(1)
	$E_{478}\mathbf{N}_{479}$	gAGaAT	(1)
	$E_{478}\mathbf{N}_{479}$	gAa aAc	(2)
	$E_{478}\mathbf{T}_{479}$	gAa aCc	(4)
	$E_{478}\mathbf{T}_{479}$	gAG aCc	(2)
	$E_{478}\mathbf{F}_{479}$	gAG Ttc	(2)
	$E_{478}\mathbf{F}_{479}$	gAa Ttc	(4)
	$E_{478}\mathbf{Y}_{479}$	gAa TAc	(1)
	$E_{478}\mathbf{Y}_{479}$	gAG TAc	(1)
	$E_{478}\mathbf{L}_{479}$	gAa Ctc	(2)
	$E_{478}\mathbf{L}_{479}$	gAa CtA	(1)
	$E_{478}\mathbf{H}_{479}$	gAG CAc	(1)
	$E_{478}\mathbf{H}_{479}$	gAa CAc	(1)
	$E_{478}\mathbf{M}_{479}$	gAa atG	(1)
	$E_{478}\mathbf{C}_{479}$	gAa TGc	(3)
	$E_{478}\mathbf{A}_{479}$	gAa GCA	(1)
	$E_{478}\mathbf{Q}_{479}$	gAG CAA	(1)
	$E_{478}\mathbf{P}_{479}$	gAa CCc	(1)

[a] The amino acid residues that differ from the native sequence are in bold underlined. DNA sequences follow. Nucleotides in capitals indicate the changes compared to the lethal template used to prepare the library. Number between brackets referred to the number of clones selected.

Search for Intragenic Suppressors of the Mutants of the Acidic Residues. In a new attempt to isolate active suppressors of 471 and 478 lethal mutations, we built two new libraries derived from the lethal templates DN471 and EG478. Two oligonucleotides complementary to the gene segment encoding residues 468−484 were synthesized with a 10% mixture of the four nucleotides at each position. To prevent the selection of nonmutated *APS* from the template, the libraries were built starting from the lethal DN471 and EG478 templates. Two libraries of pRS314-*APS*$_{(DN471\ or\ EG478)}$, of about 40 000 clones each, were built. The sequences of a set of randomly chosen mutants were determined by DNA sequence analysis. The results showed that the libraries had no bias for mutations at particular locations. The libraries were screened in the yeast (YAL3, pGALS1315-*APS*) on glucose-containing medium. Growing colonies with white sectors were isolated. After the phenotypes were confirmed by retransformation of the (YAL3, pGALS1315-*APS*) strain, the DNA were sequenced. Fifty-eight clones were isolated from the DN471 library, and 50 from the DG478 library. Thirty-four clones from the DN471 library exhibited native sequences with reversions to the original D471 residue. Twenty-five clones from the EG478 library exhibited reversions to the original Glu residue. The other clones selected in the two libraries displayed one or two mutations in addition to the acidic residue reversion (Table 4). Thus, the single or double mutations selected can be considered as silent mutations or as mutations with effects compatible with the cell life. Interestingly, one double mutant DE471+FY473 was selected in the DN471 library (Table 4). As DE471 is a mutation with a lethal effect, FY473 can be considered as an intragenic suppressor of the DE471 mutation. FY473 was also found in three other clones exhibiting a true D471 reversion. Two were single mutants FY473, and one was a double mutant FY473+MI474. To understand the suppression phenomenon of the DE471+FY473 mutant, we overexpressed the mutated gene in *E. coli* and purified the protein.

The FY473 Mutation Partially Restores the DE471 Catalytic Effect. Kinetic analysis was performed on the mutated protein and was compared to the DE471 mutant and to the native AspRS (Table 5). Mutant DE471 was strongly impaired in its catalytic properties. Aminoacylation was decreased by 2 orders of magnitude, and the amino acid activation rate was 5-fold reduced. Significant drops of ATP and aspartate affinities were also observed. The pseudorevertant DE471+FY473 exhibited a significant restoration of the aminoacylation activity compared to original DE471 mutant. The charging rate reached one-fifth of the original wild type activity, which probably explained the growth phenotype. The 2-fold decrease of the amino acid activation rate compared to the DE471 activity was unexpected. However, it is compatible with the fact that the rate-limiting step of the global reaction is the charging step, and significant rate decreases of the first step of amino acid activation can occur without affecting the global aminoacylation step (*4*).

Table 4: Sequences of the Active AspRS Variants that Were Selected in the DN471- and EG478-Degenerated Libraries[a]

> > > β strand > > > >									*turn*		*> > > > β strand > > > >*				
N$_{468}$	***S*$_{469}$**	*Y*$_{470}$	*D*$_{471}$	*F*$_{472}$	*F*$_{473}$	*M*$_{474}$	*R*$_{475}$	*G*$_{476}$	*E*$_{477}$	***E*$_{478}$**	*I*$_{479}$	*L*$_{480}$	*S*$_{481}$	***G*$_{482}$**	***A*$_{483}$**	*Q*$_{484}$
S$_{468}$																
	F$_{470}$															
	E$_{471}$	Y$_{473}$														
		I$_{472}$														
		V$_{472}$														(2)
		L$_{472}$														
		C$_{472}$														(2)
		I$_{472}$	S$_{473}$													
		V$_{472}$		I$_{474}$												
		C$_{472}$		I$_{474}$												
		L$_{472}$			T$_{475}$											
		C$_{472}$				R$_{476}$										
		C$_{472}$				G$_{476}$										
			Y$_{473}$													(2)
			I$_{473}$													
			V$_{473}$													
			L$_{473}$													(2)
			C$_{473}$													
			Y$_{473}$	I$_{474}$												
			V$_{473}$		T$_{475}$											
				I$_{474}$												
				V$_{474}$												
				L$_{474}$												
				L$_{474}$		D$_{476}$										
				K$_{475}$												
					T$_{475}$											
					M$_{475}$											(3)
					W$_{475}$											
						S$_{476}$										
						D$_{476}$										
							A$_{477}$									
							K$_{477}$									
							A$_{477}$					S$_{480}$				
											V$_{479}$					
											L$_{479}$					
											F$_{479}$					
											T$_{479}$					
											D$_{479}$					
												V$_{480}$				
												M$_{480}$				
												S$_{480}$				
													T$_{481}$			
																H$_{484}$
N$_{468}$	***S*$_{469}$**	*Y*$_{470}$	*D*$_{471}$	*F*$_{472}$	*F*$_{473}$	*M*$_{474}$	*R*$_{475}$	*G*$_{476}$	*E*$_{477}$	***E*$_{478}$**	*I*$_{479}$	*L*$_{480}$	*S*$_{481}$	***G*$_{482}$**	***A*$_{483}$**	*Q*$_{484}$

[a] One mutant per line. Only mutated residues are indicated. Numbers between brackets refer to the number of clones selected when superior to one. On the top and the bottom, the native sequence is indicated in italic; bold-underlined residues were not found mutated. The suppressor E471+Y473 is boxed.

Table 5: Growth Phenotypes and Catalytic Properties of the Mutated AspRS Proteins

		aminoacylation		ATP-PPi exchange		
	growth phenotype	k_{cat} s^{-1}	K_m ATP μM	k_{cat} s^{-1}	K_m aspartate mM	K_d $tRNA^{Asp}$ 10^{-8} M
wild-type	viable	0.83	30	27	2.5	3.0
DE471	lethal	0.007	1750	6.1	19.6	2.7
DE471+FY473	viable	0.147	2000	3.4	8.3	3.0

DISCUSSION

Two Acidic Residues Occupy Strategic Positions in the ATP Binding Site and Are Functionally Irreplaceable. In the class II synthetases, the ATP molecule adopts a specific U-shaped conformation, with the pyrophosphate moiety of the molecule bent toward the adenine ring (*4*, *13*). The bent conformation is stabilized by hydrogen bonds involving several class II conserved residues belonging to motifs 2 and 3. The γ-phosphoryl group is held by several hydrogen bonds

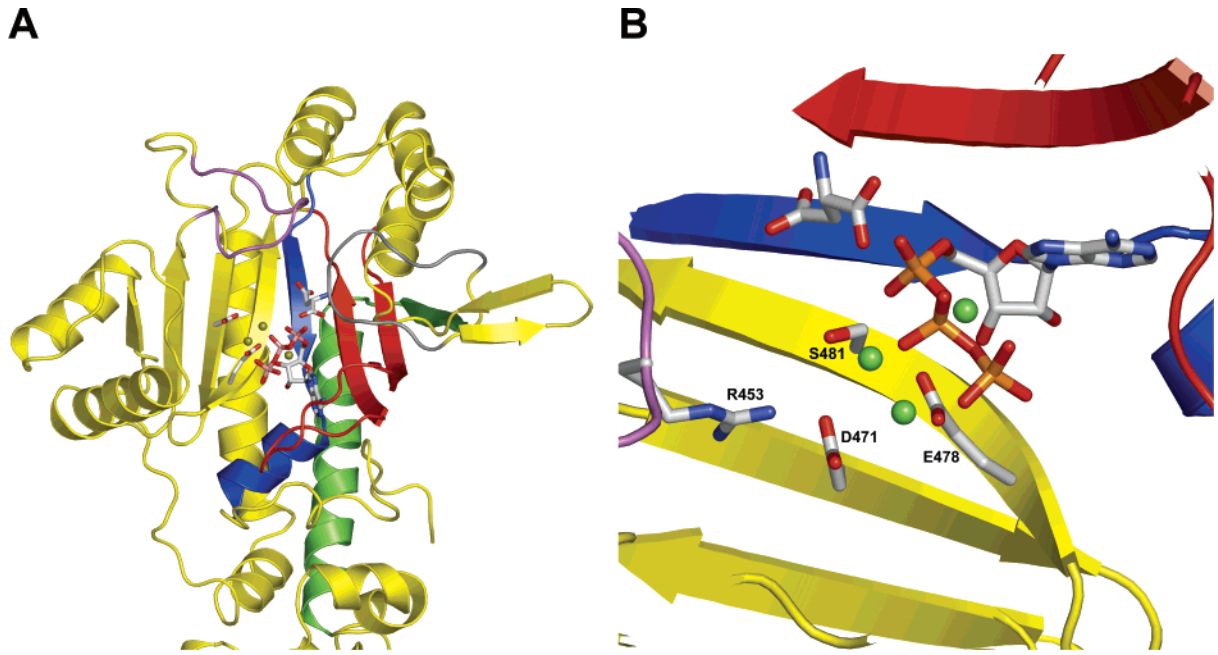

FIGURE 1: (A) Overview of the active site of one AspRS monomer showing the ATP molecule, the amino acid substrate (Asp), the two acidic residues (D471, E478), and the three magnesium ions (shown as olive spheres) The three signature motifs characteristic of class II AaRS motifs are shown in green (motif 1), red (motif 2), and blue (motif 3). The flipping loop (in gray) and the histidine loop (in magenta) are also displayed (Figures 1 and 2 were drawn with PyMol (*35*)). (B) View of the Mg^{2+} binding site of yeast AspRS. The ATP molecule is shown in its bent conformation as well as the three typical class II Mg^{2+} ions (shown as green spheres). The two acidic residues are shown as well as R453 and S481 two other key residues of the Mg^{2+} binding site. The three Mg^{2+} ions and the Asp molecule are from the structure of *P. kodakaraensis* KOD AspRS (*12*).

involving the NH groups of the class II invariant Arg residue of motif 3, while the binding of the α-phosphoryl group involves the invariant Arg residue from motif 2. In addition, the bent conformation is stabilized by three hexacoordinated magnesium ions, one of them bridging the α-phosphate and β-phosphate and the two others interacting with the β-phosphate and γ-phosphate (*12*, *13*, *30*, *31*). Magnesium ions contribute to the withdrawal of electrons from the phosphate groups, but their contribution to the reaction is also structural. They stabilize the U-shaped conformation, bind the N7 atom of adenine, and maintain the β-phosphate group in an optimal position for the in-line attack on the α-phosphate by the amino acid carboxylate group, and facilitate the release of the pyrophosphate group. On the basis of Mg^{2+} functional requirement studies, it has been postulated that the presence of three Mg^{2+} ions is distinctive of class II synthetases (*32*). However, histidyl-tRNA synthetase is an exception to this rule and contains only two divalent ions, while a specific additional Arg residue plays the role of the missing Mg^{2+} ion (*14*, *33*, *34*). Differences in the binding strength of the Mg^{2+} have also been detected. The Mg^{2+} that bridges the α- and β-phosphate is stronger in SerRS and AsnRS (*13*, *30*), whereas the Mg^{2+} that bridges the β- and γ-phosphate is stronger in AspRS (*12*). In the known structures of binary complexes ATP:class II synthetase two acidic residues are involved in the coordination of the Mg^{2+} ions. They are located in two adjacent strands of the antiparallel β-sheet and interact with two Mg^{2+} ions. In yeast AspRS, these residues are D471 and E478 (Figure 1). These two acidic residues are essentially conserved in all class II synthetases. These residues were not identified as class II signature elements probably because the adjacent sequences are highly variable. With the increasing number of available 3D structures, it becomes apparent that two acidic groups are extremely conserved at this level of the active site. Early work on yeast AspRS showed, by site-directed experimentation, that these two amino acids play a crucial role in ATP and amino acid binding as well as amino acid activation and tRNA charging (*4*, *16*). Since ATP and aspartate binding are linked, incorrect binding of ATP may explain the effect on the aspartate binding. Thus, the mutation of the acidic residues indirectly affects the ATP binding through the Mg^{2+} ions binding. Mutagenesis showed that conservative changes have a strong negative impact on the activity. The enzyme did not tolerate changes of the side chain length or substitution of the acidic group by an amido group. Removal of the side chain by Ala mutagenesis also produced an inactive enzyme (Table 1). Altogether, these results further suggest if not confirm that these two acidic residues play an essential role in the accurate positioning of the Mg^{2+} ions and indirectly of the ATP molecule.

Despite this body of data, we examined whether these acidic residues can be replaced by others that might produce a rearrangement of the Mg^{2+} binding site and give an active enzyme. We considered as active enzymes those with activity levels compatible to cell growth, and thus we used yeast genetics and genetic screens to isolate active AspRS. In the present work, we planned to screen all the possible substitutions at these positions, and thus we designed a positive selection based on the promoter GALS involved in the galactose metabolism. Compared to the plasmid-shuffling method previously used (*16*), the GALS procedure is based on the arrest of the cell growth following the shut down of the AspRS expression on glucose medium. Clones that express active AspRS molecules in trans can easily be isolated from a library simply by plating on the appropriate

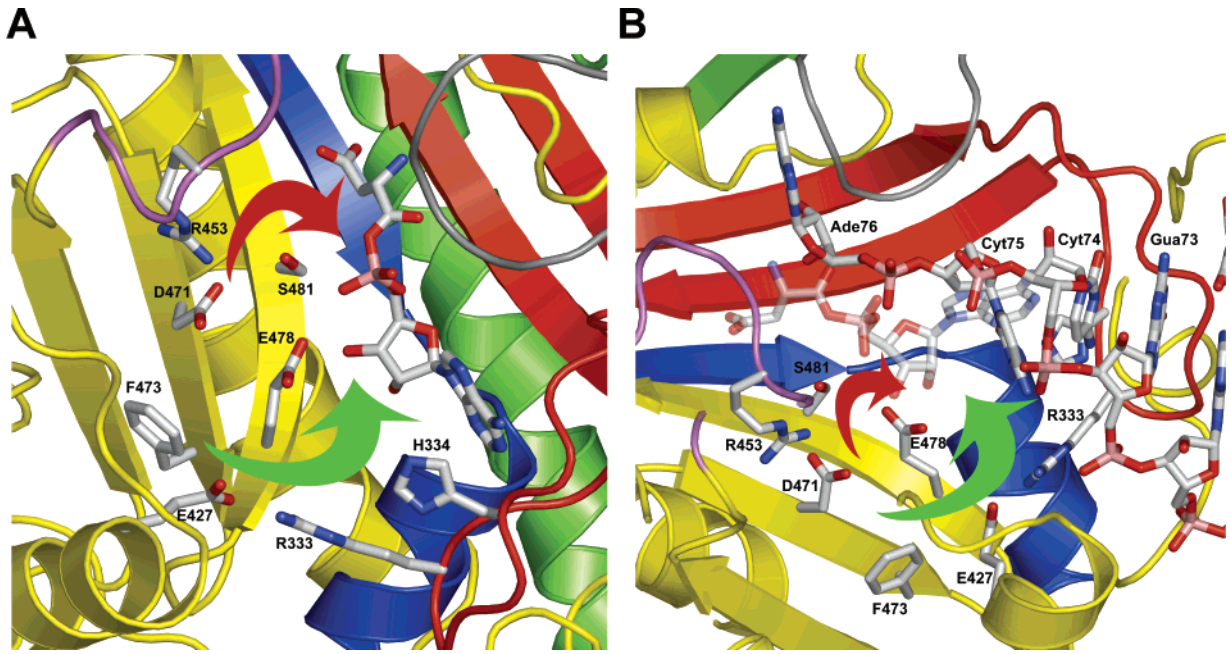

FIGURE 2: (A) Overview of the AspRS active site showing the adenylate molecule and illustrating the hypothetical pathway of enzyme reactivation for the DE471+FY473 pseudo-revertant. Mutation DE471 affects the ATP and aspartate binding and is followed by catalytic effects on the activation and charging steps (pathway schematized by a red arrow). This inactivation can be reverted by a single FY473 change, and kinetic properties of the DE471+FY473 AspRS mutant reveal a partial recovery of the charging rate without improving the binding of ATP and aspartate or the amino acid activation rate. Another pathway (schematized by a green arrow) may be used to balance the modifications induced by the first mutation (DE471). The FY473 mutation may produce structural changes of the proteins that will include the alteration of the salt bridge found in the wild type AspRS between E427 and R333, resulting in the conformational change of the side chain of H334 leading to a slightly different productive position of the tRNA acceptor (not shown here for clarity). (B) The tRNA acceptor end has been added. The red arrow schematizes the hypothetical pathway for enzyme inactivation, while the green arrow schematizes the reactivation produced by the (DE471+FY473) pseudo-revertant.

medium. The libraries expressing the mutated AspRS were designed to randomly mutate the acidic residue and its adjacent neighbor. The screening efficiency was significantly increased when using mutated templates of lethal AspRS genes. Thus, the clones that were able to grow necessarily reverted the lethal effect by one or several mutations. The sequencing of about one hundred clones revealed a strict reversion toward the native D471 and E478 residues. Thus, despite the use of a partially degenerate library, the in vivo assay only selected reversions to the native acidic residue. However, they were accompanied by extensive changes at the adjacent nonconserved position, which greatly contribute to the validation of the approach and verify the quality of the libraries. At position 472, the hydrophopic Phe residue was replaced by other hydrophobic residues or by small polar residues. We suggest that the hydrophobic pocket found at that level of the protein could easily accept other hydrophobic residues, as well as small polar residues. Residue I479 also participates in the hydrophobic pocket stabilization. Although an hydrophobic residue is always found at that level in the AspRS sequences, we selected a panel of 12 different amino acids substitutions, comprising hydrophobic and small polar residues, but also bigger His, Asn, and Gln residues. The fact that the protein environment can accommodate these residues supposes that the protein can tolerate some structural alterations at this level of the central β-sheet. The main function of the hydrophobic environment is to maintain the last strands of the β-sheet. These elements are too distant to be involved in direct substrate binding. Rather, they connect several helices and loops that interact with the sugar−phosphate backbone of the tRNA acceptor arm.

FY473, an Intragenic Suppressor of DE471 Restores the Aminoacylation Activity. It was previously shown that the DE471 mutation inactivates AspRS by k_{cat} and K_m effects. These pleiotropic effects suggest that mutation DE471 affects the first step of ATP and aspartate binding and is followed by catalytic effects on the activation and charging steps. This has been confirmed by the analysis of several crystal structures of three AspRS (*4*, *6*, *12*). Analysis of the 3D structures revealed that D471 is involved in two molecular interactions. On one side, this invariant acidic residue builds up two of the three Mg^{2+} binding sites as it interacts by a water-mediated interaction with those cations in the ATP-bound conformation of AspRS (*12*). On the other side, D471 interacts with the so-called histidine loop, which is implicated in the aspartate and aspartyl-adenylate recognition (*2*). The sequence of this loop splits the AspRS family into two classes: (i) the first one contains all eubacterial AspRS and is characterized by a His residue in first position of the consensus sequence H(H/N)λF(T/S), and (ii) the second one contains all eukaryotic and archaebacterial AspRS and is characterized by an Arg or Lys residue in first position of the consensus motif (R/K)PFYY. The crystal structures of yeast AspRS and *P. kodakaraensis* KOD AspRS have shown that D471 interacts by a direct ionic interaction with the basic residue in position 1 of the consensus motif of the histidine loop (K336 in *P. kodakaraensis* KOD AspRS and R453 in yeast AspRS, Figure 2). Such interaction is crucial as shown by the lethal effect observed with the RC453 mutation in the yeast AspRS (*16*). On the other hand, the crystal structures of *E. coli* and *T. thermophilus* AspRS have shown that the invariant aspartic acid corresponding to D471 is

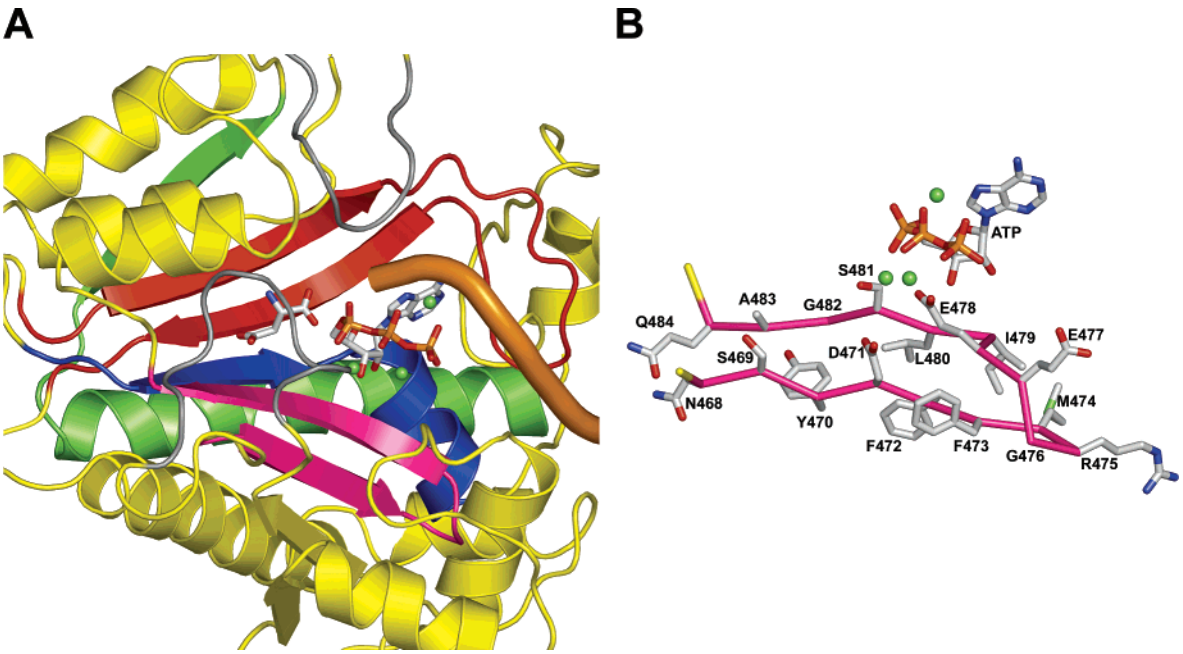

FIGURE 3: (A) Overview of the active site of one AspRS monomer showing the location in space of the AspRS variants that were selected in the DN471- and EG478-degenerated libraries. The mutated peptide is shown in pink (from residues 469 to 484). It belongs to two antiparallel strands connected by a loop. The ATP molecule, the aspartate substrate, as well as the three typical class II Mg^{2+} ions are also shown. The tRNA backbone is drawn with its phosphate chain traced with a thick orange line (the CCA end is only shown here). (B) Simplified view of the mutated two strands with the wild-type residues. The main chain atoms have been omitted. S469, G482, and A483 are part of the aspartate substrate binding site floor and cannot be replaced without any drastic effect on the enzyme activity. Y470, F472, M474, I479, L480 are part of the hydrophobic core of the enzyme.

linked by a water-mediated interaction with the first conserved histidine (H448 in *E. coli* AspRS and H442 in *T. thermophilus* AspRS) of the histidine loop. Moreover, the analyses of all known AspRS sequences in both classes of AspRS suggest that these two types of interactions can be generalized to all eubacterial, eukaryotic, and archaebacterial AspRS. Altogether, these structural and phylogenetic data explain why both ATP and aspartate binding are affected on DE471 mutation, as well as adenylate and aminoacyl-tRNA formation.

The experimental data presented in this work show that this inactivation can be reverted by a single FY473 change, as kinetic properties of the pseudo-revertant DE471+FY473 displays a partial recovery of the charging rate without changing significantly the binding of ATP and aspartate or the amino acid activation rate. This result suggests that the pseudo-revertant DE471+FY473 leads to a rearrangement of the atoms, which are suitable enough for a productive reaction. The fact that only the charging rate was restored by the reversion suggests that the FY473 mutation compensates for the structural defect induced by the DE471 mutation by inducing a slightly different position of the tRNA acceptor end in the active site of the enzyme. The modifications induced by the DE471+FY473 mutants may produce an alternate atomic configuration, which stabilizes the transition state of the second step of the aminoacylation reaction and therefore explains the observed kinetic parameters.

Examination of the crystal structure suggests a pathway, which can be used to balance the modifications induced by the first mutation (DE471) by a different position of the tRNA acceptor end. The FY473 mutation may produce structural changes of the proteins that will include the alteration of the salt bridge found in the wild-type AspRS between E427 and R333, resulting in the conformational change of the side chain of H334. H334, a motif 2 residue of the protein, interacts with the O2 atom of Cyt75 of the tRNA (Figure 2).

Several substitutions of the H334 residue have been done (*4*, *16*, *24*). Bulky Lys, Tyr, or smaller Ala substitutions drastically decrease the charging rate and can generate lethality. On the other hand, the Arg, Asn, and Gln replacements exhibit moderate effects on the acylation reaction, demonstrating that a productive interaction with the tRNA can occur with residues exhibiting different side chain lengths. These data also suggest that displacement of H334, as hypothesized in the double DE471+FY473 mutant, may also generate an enzyme capable of tRNA charging.

A modification of the conformation of E427 may also induce structural changes of three neighboring residues S423, T424, and K428 located at the beginning of helix H6. These residues are involved in the correct positioning of the tRNA on the enzyme, interacting with the tRNA phosphate groups of residues Ade72, Gua73.

Selection of Active Variants in Degenerated Libraries: A Tool to Estimate the Essential Character of Amino Acid Residues. We have used a strategy of selection of active AspRS molecules starting from lethal templates. For this, degenerated libraries were built and screened in an inducible *APS* yeast strain. Most of the viable clones exhibit true reversions of the lethal mutations, and additionally, silent mutations, which reflect the natural variation observed at these positions. In addition, one of these silent mutations was also found to be a suppressor of the original lethal mutation. This was the case of FY473 substitution that was isolated as a single mutation and double mutant in the pseudo-revertant DE471+FY473.

Moreover, the distribution of silent mutations can be examined as new functional data in the light of the 3D structure. Results of Table 4 show that only four positions could not be mutated as single or double mutants, and thus are suspected to be essential and irreplaceable. These are S469, E478, G482, and A483. Among these residues, three were previously isolated as lethal mutations: SP469, EG478, and AV483 (*16*). Interestingly, only residue 478 was studied by site-directed mutagenesis, because of its interaction with Mg^{2+}. The study of the small S469, G482, and A483 residues was omitted because they were not directly interacting with the substrates. This way, we show that the in vivo studies can also reveal the importance of essential residues, which participate in the enzyme architecture. S469, G482, and A483 are part of the floor of the active site where the ATP molecule sits (Figure 3). They cannot be replaced without any deleterious effects on the enzyme activity, probably by the steric effect generated by any other mutation. Sequences analysis show that E478 and G482 are strictly invariant in all AspRS, whereas certain variations can be observed for S469 and A483. Other residues such as Y470 and S481 were only mutated once, in agreement with their structural function and sequence conservation (YF470 and ST481).

However, one of the limitations of this approach consists of the library quality and mutation dosage. The presence of multiple mutants raises questions about the role of individual mutations. An obvious advantage resides in the suppression role that can play a second mutation on the first one. The DE471+FY473 is a typical example. Nevertheless, too many mutations can make the analysis complex and dilute crucial information resulting from single mutant analysis.

ACKNOWLEDGMENT

We want to express our gratitude to Dr. Jean Gangloff for stimulating discussions and Dr. A. Camasses for advice and suggestions. We are grateful to Paul Beglan for careful reading of the manuscript.

REFERENCES

1. Eriani, G., Delarue, M., Poch, O., Gangloff, J., and Moras, D. (1990) Partition of tRNA synthetases into two classes based on mutually exclusive sets of sequence motifs, *Nature 347*, 203−206.
2. Eiler, S., Dock-Bregeon, A., Moulinier, L., Thierry, J., and Moras, D. (1999) Synthesis of aspartyl-tRNA^{Asp} in *Escherichia coli* − a snapshot of the second step, *EMBO J. 18*, 6532−6541.
3. Perona, J. J., Rould, M. A., and Steitz, T. A. (1993) Structural basis for transfer RNA aminoacylation by *Escherichia coli* glutaminyl-tRNA synthetase, *Biochemistry 32*, 8758−8771.
4. Cavarelli, J., Eriani, G., Rees, B., Ruff, M., Boeglin, M., Mitschler, A., Martin, F., Gangloff, J., Thierry, J. C., and Moras, D. (1994) The active site of yeast aspartyl-tRNA synthetase: structural and functional aspects of the aminoacylation reaction, *EMBO J. 13*, 327−337.
5. Ruff, M., Krishnaswamy, S., Boeglin, M., Poterszman, A., Mitschler, A., Podjarny, A., Rees, B., Thierry, J. C., and Moras, D. (1991) Class II aminoacyl transfer RNA synthetases: crystal structure of yeast aspartyl-tRNA synthetase complexed with tRNA^{Asp}, *Science 252*, 1682−1689.
6. Poterszman, A., Delarue, M., Thierry, J.-C., and Moras, D. (1994) Synthesis and recognition of aspartyl-adenylate by *Thermus thermophilus* aspartyl-tRNA synthetase, *J. Mol. Biol. 244*, 158−167.
7. Cavarelli, J., Rees, B., Ruff, M., Poterszman, A., Thierry, J.-C., and Moras, D. (1992) in *Structural Tools for the Analysis of Protein-Nucleic Acid Complexes*, pp 287−298, Birkhäuser Verlag, Basel.
8. Briand, C., Poterszman, A., Eiler, S., Webster, G., Thierry, J., and Moras, D. (2000) An intermediate step in the recognition of tRNA^{Asp} by aspartyl-tRNA synthetase, *J. Mol. Biol. 299*, 1051−1060.
9. Moulinier, L., Eiler, S., Eriani, G., Gangloff, J., Thierry, J. C., Gabriel, K., McClain, W. H., and Moras, D. (2001) The structure of an AspRS-tRNA^{Asp} complex reveals a tRNA-dependent control mechanism, *EMBO J. 20*, 5290−5301.
10. Sauter, C., Lorber, B., Cavarelli, J., Moras, D., and Giege, R. (2000) The free yeast aspartyl-tRNA synthetase differs from the tRNA^{Asp}-complexed enzyme by structural changes in the catalytic site, hinge region, and anticodon-binding domain, *J. Mol. Biol. 299*, 1333−1344.
11. Rees, B., Webster, G., Delarue, M., Boeglin, M., and Moras, D. (2000) Aspartyl tRNA-synthetase from *Escherichia coli*: Flexibility and adaptability to the substrates, *J. Mol. Biol. 299*, 1157−1164.
12. Schmitt, E., Moulinier, L., Fujiwara, S., Imanaka, T., Thierry, J. C., and Moras, D. (1998) Crystal structure of aspartyl-tRNA synthetase from *Pyrococcus kodakaraensis* KOD: archaeon specificity and catalytic mechanism of adenylate formation, *EMBO J. 17*, 5227−5237.
13. Belrhali, H., Yaremchuk, A., Tukalo, M., Berthet-Colominas, C., Rasmussen, B., Bösecke, P., Diat, O., and Cusack, S. (1995) The structural basis for seryl-adenylate and Ap4A synthesis by seryl-tRNA synthetase, *Structure 3*, 341−352.
14. Arnez, J. G., Augustine, J. G., Moras, D., and Francklyn, C. S. (1997) The first step of aminoacylation at the atomic level in histidyl-tRNA synthetase, *Proc. Natl. Acad. Sci. U.S.A. 94*, 7144−7149.
15. Patterson, T. A., Costantino, N., Dasgupta, S., and Court, D. L. (1993) Improved bacterial hosts for regulated expression of genes from λ PL plasmid vectors, *Gene 132*, 83−87.
16. Ador, L., Camasses, A., Erbs, P., Cavarelli, J., Moras, D., Gangloff, J., and Eriani, G. (1999) Active site mapping of yeast aspartyl-tRNA synthetase by *in vivo* selection of enzyme mutations lethal for cell growth, *J. Mol. Biol. 288*, 231−242.
17. Sellami, M., Chatton, B., Fasiolo, F., Dirheimer, G., and Gangloff, J. (1986) Nucleotide sequence of the gene coding for yeast cytoplasmic aspartyl-tRNA synthetase (*APS*); mapping of the 5′ and 3′ termini of AspRS mRNA, *Nucleic Acids Res. 14*, 1657−1666.
18. Sikorski, R. S., and Hieter, P. (1989) A system of shuttle vectors and yeast host strains designed for efficient manipulation of DNA in *Saccharomyces cerevisiae*, *Genetics 122*, 19−27.
19. Mumberg, D., Muller, R., and Funk, M. (1994) Regulatable promoters of *Saccharomyces cerevisiae*: comparison of transcriptional activity and their use for heterologous expression, *Nucleic Acids Res. 22*, 5767−4768.
20. Alexeyev, M. F. (1995) Three kanamycin resistance gene cassettes with different polylinkers, *Biotechniques 18*, 52−56.
21. Koshland, D., Kent, J. C., and Hartwell, L. H. (1985) Genetic analysis of the mitotic transmission of minichromosomes, *Cell 40*, 393−403.
22. Ausubel, F. M., Brent, R., Kingston, R. E., Moore, D. D., Smith, J. A., Seidman, J. G., and Struhl, K. (1987) *Current Protocols in Molecular Biology*, Wiley-Interscience, New York.
23. Kunkel, T. A. (1985) Rapid and efficient site-specific mutagenesis without phenotypic selection, *Proc. Natl. Acad. Sci. U.S.A. 82*, 488−492.
24. Eriani, G., and Gangloff, J. (1999) Yeast aspartyl-tRNA synthetase residues interacting with tRNA^{Asp} identity bases connectively contribute to tRNA^{Asp} binding in the ground and transition-state complex and discriminate against non-cognate tRNAs, *J. Mol. Biol. 291*, 761−773.
25. Boeke, J. D., LaCroute, F., and Fink, G. R. (1984) A positive selection for mutants lacking orotidine-5′-phosphate decarboxylase activity in yeast: 5-fluoro-orotic acid resistance, *Mol. Gen. Genet. 197*, 345−346.
26. Courtney, M., Buchwalder, A., Tessier, L. H., Jaye, M., Benavente, A., Balland, A., Kohli, V., Lathe, R., Tolstoshev, P., and Lecocq, J. P. (1984) High-level production of biologically active human α1-antitrypsin in *Escherichia coli*, *Proc. Natl. Acad. Sci. U.S.A. 81*, 669−673.
27. Prévost, G., Eriani, G., Kern, D., Dirheimer, G., and Gangloff, J. (1989) Study of the arrangement of the functional domains along the cytoplasmic aspartyl-tRNA synthetase, *Eur. J. Biochem. 180*, 351−358.
28. Eriani, G., Cavarelli, J., Martin, F., Dirheimer, G., Moras, D., and Gangloff, J. (1993) Role of dimerization in yeast aspartyl-tRNA

synthetase and importance of the class II invariant proline, *Proc. Natl. Acad. Sci. U.S.A. 90*, 10816−10820.
29. Eriani, G., Prevost, G., Kern, D., Vincendon, P., Dirheimer, G., and Gangloff, J. (1991) Cytoplasmic aspartyl-tRNA synthetase from *Saccharomyces cerevisiae*. Study of its functional organisation by deletion analysis, *Eur. J. Biochem. 200*, 337−343.
30. Berthet-Colominas, C., Seignovert, L., Hartlein, M., Grotli, M., Cusack, S., and Leberman, R. (1998) The crystal structure of asparaginyl-tRNA synthetase from *Thermus thermophilus* and its complexes with ATP and asparaginyl-adenylate: the mechanism of discrimination between asparagine and aspartic acid, *EMBO J. 17*, 2947−2960.
31. Desogus, G., Todone, F., Brick, P., and Onesti, S. (2000) Active site of lysyl-tRNA synthetase: structural studies of the adenylation reaction, *Biochemistry 39*, 8418−8425.
32. Airas, R. K. (1996) Differences in the magnesium dependences of the class I and class II aminoacyl-tRNA synthetases from *Escherichia coli*, *Eur. J. Biochem. 240*, 223−231.
33. Aberg, A., Yaremchuk, A., Tukalo, M., Rasmussen, B., and Cusack, S. (1997) Crystal structure analysis of the activation of histidine by *Thermus thermophilus* histidyl-tRNA synthetase, *Biochemistry 36*, 3084−3094.
34. Arnez, J. G., Flanagan, K., Moras, D., and Simonson, T. (1998) Engineering and Mg^{2+} site to replace a structurally conserved arginine in the catalytic center of histidyl-tRNA synthetase by computer experiments, *Proteins 32*, 362−380.
35. DeLano, W. L. (2002) The PyMOL Molecular Graphics System, on the World Wide Web, http://www.pymol.org.

BI049617+